

Transport approach to two-qubit quantum state tomography

Jeanne Bourgeois^{1,2,3}, Gianmichele Blasi¹ and Géraldine Haack¹

¹*Department of Applied Physics, University of Geneva, 1211 Geneva, Switzerland*

²*Institute of Physics, Ecole Polytechnique Fédérale de Lausanne (EPFL), CH-1015 Lausanne, Switzerland*

³*Center for Quantum Science and Engineering, Ecole Polytechnique Fédérale de Lausanne (EPFL), CH-1015 Lausanne, Switzerland*

(Dated: January 27, 2025)

Quantum state tomography (QST) is a central task for quantum information processing, enabling quantum cryptography, computation, and state certification. Traditional QST relies on projective measurements of single- and two-qubit Pauli operators, requiring qubits to be isolated from environmental dissipation. In this work, we demonstrate that measuring currents and associated transport quantities flowing through a two-qubit system between two terminals biased in temperature or voltage are sufficient to perform complete QST of the open quantum system. This transport approach requires minimal knowledge of the system-environment couplings and of the parameters setting the system's dynamics, accessible in state-of-the-art solid-state experiments via spectroscopic measurements for instance. Our findings are analytical, offering comprehensive insights into the underlying processes. As a direct consequence of our approach, we are able to provide a transport-based entanglement measure to certify the presence of quantum correlations, expressing the concurrence in terms of currents and correlations functions only.

Introduction.— Demonstrating the presence of entanglement between two qubits is one of the key milestones for efficient quantum information processing, requiring the possibility to achieve quantum state tomography (QST) of multiple qubits [1–3]. Seminal experimental works based on different platforms have realized QST involving one to multiple qubits, with superconducting qubits [4, 5], trapped ions [6, 7] and NV centers [8, 9]. QST protocols are typically based on linear inversion of local and global Pauli observables directly related to elements of the density operator, and on numerical optimization through various statistical estimators [10, 11] or classical shadow algorithms [12]. Remarkably, QST protocols contributed very recently to demonstrate loophole-free violation of Bell inequalities using solid-state qubits [13–15], and are starting to be explored from the point of view of novel advanced numerical techniques [16].

While uncontrolled dissipation leading to noise is considered as detrimental in the above experimental achievements, its role towards quantum information processing and its applications has considerably changed in the past two decades. On one hand, engineered dissipation has been shown to constitute an alternative lever for generating and manipulating quantum resources, through stabilization of entangled states in decoherence-free subspaces [17–21] and autonomous quantum error correction codes [22–24]. On the other hand, it remains an open question whether uncontrolled dissipation, in the form of heat from a thermodynamics point of view, can also constitute a resource for quantum information processing. It has triggered an increased interest over the last two decades, leading to theoretical proposals for autonomous generation of entanglement in open quantum systems setups [25–32]. In particular, the successful functioning of an entanglement engine was shown to be conditioned on a minimal critical charge or heat current flowing through two interacting qubits in a two-terminal device [33–35]. This

result suggested a connection between transport properties of an open quantum system and its quantum state.

In this work, we address the fundamental question whether transport measurements, in the form of current averages and fluctuations, can provide a complete characterization of the state of an open quantum system. Considering a model of two interacting qubits embedded within a two-terminal device subject to a voltage or temperature bias, we show that QST of the two-qubit system can be achieved exclusively based on transport quantity measurements. We provide a complete analytical description for the case of two interacting qubits weakly coupled to two Markovian reservoirs, within a master equation approach to assess their quantum dynamics. We derive exact relations between transport quantities - currents, time-derivatives of the currents, and current correlation functions - and density operator's elements. These relations depend on the system's internal dynamics and on the system-environment couplings. Furthermore, we show that this transport-based tomography scheme only requires the *a priori* knowledge of the system-bath coupling strengths. All other parameters, including those governing the system's unitary dynamics and local pure dephasing, can be extracted from additional transport-based quantities. Importantly, these results allow us to express the concurrence, an entanglement measure, in terms of transport quantities only. This further establishes fundamental connections between the quantum state of an open quantum system and observables measured in the environment, and opens the way to novel practical QST protocols for open quantum systems.

Theoretical framework.— We consider an open quantum system made of two interacting qubits (referred to as left “*L*” and right “*R*”) with Hamiltonian \hat{H}_S and density operator $\hat{\rho}$, that can be subject to pure dephasing, and

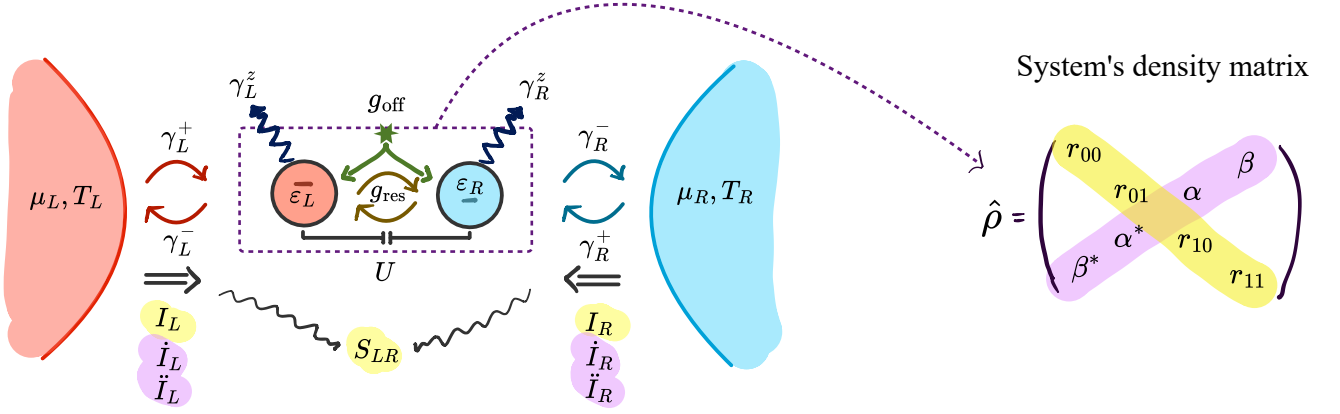


FIG. 1. Illustration of the tomography of a bipartite open quantum system through the measurement of transport observables. A system of two interacting qubits (dashed box), described by its density matrix ρ , is subject to dissipation through its coupling to two thermal baths ($\gamma_{L/R}^{\pm}$), biased in temperature ($T_{L/R}$) and/or voltage ($\mu_{L/R}$), and potentially to pure dephasing ($\gamma_{L/R}^z$). The two qubits are characterized by their bare energies ($\varepsilon_{L/R}$). They can be subject to Coulomb-type (U), particle-conserving (g_{res}) and non-conserving (g_{off}) inter-qubit interactions. Measuring the current averages I_L , I_R and instantaneous cross-correlation S_{LR} determines the populations (diagonal elements) of $\hat{\rho}$, while the two first time-derivatives of the current averages, \dot{I}_L , \ddot{I}_L , \dot{I}_R and \ddot{I}_R , provide access to its coherences (anti-diagonal elements).

coupled to two thermal reservoirs, one for each qubit (left and right, respectively). The reservoirs are biased in voltage and temperature such that charge and heat currents flow through the system. Figure 1 left panel illustrates this device. The right panel introduces the density operator $\hat{\rho}$ expressed in the canonical basis of the two qubits spanned by the states $\{|00\rangle, |01\rangle, |10\rangle, |11\rangle\}$. We denote the four populations (real numbers) by $r_{00}, r_{01}, r_{10}, r_{11}$ (in yellow). Off-diagonal elements, the coherences, are complex (in purple). Assuming Markovian reservoirs weakly coupled to their respective qubits through single-particle tunneling-type interaction Hamiltonians, as well as weak inter-qubit interaction, the time evolution of the reduced density operator $\hat{\rho}$ for the two qubits is accurately captured by a local Lindblad master equation of the form [33, 36–39] ($\hbar, k_B = 1$ throughout the work):

$$\dot{\hat{\rho}} = -i[\hat{H}_S, \hat{\rho}] + \sum_{j=L,R} (\gamma_j^+ \mathcal{D}[\hat{\sigma}_+^{(j)}] + \gamma_j^- \mathcal{D}[\hat{\sigma}_-^{(j)}]) \hat{\rho} + \sum_{j=L,R} \frac{\gamma_j^z}{2} \mathcal{D}[\hat{\sigma}_z^{(j)}] \hat{\rho}, \quad (1)$$

where $\mathcal{D}[A] \bullet \equiv A \bullet A^\dagger - \{A^\dagger A, \bullet\}/2$ is the dissipator and $\{A, B\} = AB + BA$ the Poisson bracket (see Appendix A). The first dissipative terms involve the raising ($\hat{\sigma}_+^{(j)}$) and lowering ($\hat{\sigma}_-^{(j)}$) operators for qubit j , and are proportional to the rates of particles tunneling in (γ_j^+) and out (γ_j^-) of the system from and to reservoir j , respectively. They capture the dissipative dynamics induced by the thermal baths, including relaxation and loss of quantum coherence. The second dissipative terms, involving the z-Pauli jump operators $\hat{\sigma}_z^j$ and proportional to rates $\gamma_z^{(j)}$, capture pure dephasing processes contributing to

the finite coherence time of the qubits.

According to the dynamics set by Eq. (1), time-dependent currents $I_L(t)$, $I_R(t)$ and two-time current cross-correlation function $S_{LR}(t_1, t_2)$, evaluated at $t_1 = t_2 \equiv t$, can be expressed through the current superoperators $\mathcal{I}_j \bullet \equiv \gamma_j^+ \hat{\sigma}_+^{(j)} \bullet \hat{\sigma}_-^{(j)} - \gamma_j^- \hat{\sigma}_-^{(j)} \bullet \hat{\sigma}_+^{(j)}$ for $j = L, R$ (see Refs. 39 and 40):

$$I_j(t) = \text{Tr}[\mathcal{I}_j \hat{\rho}(t)], \quad (2)$$

$$S_{LR}(t) = \text{Tr}[\mathcal{I}_L \mathcal{I}_R \hat{\rho}(t)] - \text{Tr}[\mathcal{I}_L \hat{\rho}(t)] \text{Tr}[\mathcal{I}_R \hat{\rho}(t)]. \quad (3)$$

All transport quantities of interest in this work are evaluated from Eqs. (2) and (3), constituting the theoretical framework of our transport approach to QST. In the following, we demonstrate explicit reconstructions of the populations and coherences of the density operator from these quantities.

Tomography of the populations.—Applying Eq. (2) to the two-qubit system, we obtain the following expressions for the currents in the left and right reservoirs at time t :

$$I_L(t) = \gamma_L^+ (1 - n_L(t)) - \gamma_L^- n_L(t) = \gamma_L^+ - \Gamma_L n_L(t), \quad (4a)$$

$$I_R(t) = \gamma_R^+ (1 - n_R(t)) - \gamma_R^- n_R(t) = \gamma_R^+ - \Gamma_R n_R(t), \quad (4b)$$

with $\Gamma_j \equiv \gamma_j^+ + \gamma_j^-$ the total qubit-reservoir tunneling rate on side j , and $n_L \equiv \langle \hat{n}_L \rangle = r_{10} + r_{11}$ and $n_R \equiv \langle \hat{n}_R \rangle = r_{01} + r_{11}$ the average population of the left and right qubits respectively. These equations make explicit the equivalence of measuring time-resolved currents and single-qubit occupations. To access the doubly-occupied state's probability r_{11} , we follow the same pro-

cedure as above for the instantaneous current cross-correlation function at time t :

$$S_{LR}(t) = \Gamma_L \Gamma_R \left(r_{11}(t) - n_L(t) n_R(t) \right). \quad (5)$$

Equations (4a), (4b) and (5) form a set of three linear independent equations in the density matrix's diagonal elements, from which we can reconstruct all populations:

$$r_{01}(t) = -\frac{S_{LR}(t)}{\Gamma_L \Gamma_R} - \frac{I_R(t) - \gamma_R^+ I_L(t) + \gamma_L^-}{\Gamma_R \Gamma}, \quad (6a)$$

$$r_{10}(t) = -\frac{S_{LR}(t)}{\Gamma_L \Gamma_R} - \frac{I_L(t) - \gamma_L^+ I_R(t) + \gamma_R^-}{\Gamma_L \Gamma}, \quad (6b)$$

$$r_{11}(t) = \frac{S_{LR}(t)}{\Gamma_L \Gamma_R} + \frac{I_L - \gamma_L^+ I_R - \gamma_R^+}{\Gamma_L \Gamma_R}, \quad (6c)$$

with $r_{00}(t)$ being reconstructed from the trace property $\text{Tr}\{\hat{\rho}(t)\} = 1$. The set of equations (6) shows that average currents and cross-correlated noise are sufficient to determine the populations of a two-qubit system at any given time, given that the couplings $\gamma_{L/R}^\pm$ are known *a priori*. This assumption is consistent with state-of-the-art experimental setups, as discussed in the perspectives and conclusion of this work. Interestingly, although the evolution of every density matrix element ρ_{ij} depends on the whole dynamics induced by the unitary evolution and the dissipators, at a fixed time t , the expressions for the currents $I_L(t)$, $I_R(t)$, and noise $S_{LR}(t)$ depend solely on the populations $r_{ij}(t)$. As a result, no information about coherences can be obtained from them, and additional transport measurements are required to reconstruct the coherences.

Tomography of the coherences.— To access the quantum coherences of $\hat{\rho}$, we propose to exploit time-derivatives of

the left and right currents, which depend on the unitary dynamics induced by the system's Hamiltonian H_S . This choice is motivated by two key reasons. First, they do not involve additional experimental challenges as compared to measuring time-resolved average currents needed for the populations. Second, these quantities vanish in the steady-state regime, making transport-based tomography particularly simple and elegant at long times.

To illustrate our proposal, we consider a generic Hamiltonian for two-qubit systems that induces a coupled dynamics for the diagonal and off-diagonal elements of $\hat{\rho}$:

$$\hat{H}_S = \varepsilon_L \hat{n}_L + \varepsilon_R \hat{n}_R + U \hat{n}_L \hat{n}_R + (g_{\text{res}} \hat{\sigma}_+^{(L)} \hat{\sigma}_-^{(R)} + g_{\text{off}} \hat{\sigma}_+^{(L)} \hat{\sigma}_+^{(R)}) + h.c. \quad (7)$$

The energies $\varepsilon_{L/R}$ set the bare energies of the qubits L/R , the energy U captures on-site interactions (like Coulomb interactions for charge qubits), while the energies g_{res} and g_{off} set resonant (particle-conserving) and off-resonant (particle-non-conserving) interactions respectively and are supposed real without loss of generality. Injecting the time-evolution equation (1) into the expressions for the average currents (4a) and (4b), we obtain expressions for the first and second time-derivatives of the currents in terms of density-matrix elements, that we can further manipulate to express the real and imaginary parts of the coherences in terms of transport quantities only:

$$-4 g_{\text{res}} \text{Im}(\alpha) = \frac{\dot{I}_L}{\Gamma_L} + I_L - \frac{\dot{I}_R}{\Gamma_R} - I_R, \quad (8a)$$

$$-4 g_{\text{off}} \text{Im}(\beta) = \frac{\dot{I}_L}{\Gamma_L} + I_L + \frac{\dot{I}_R}{\Gamma_R} + I_R \quad (8b)$$

and

$$-4 g_{\text{res}} \delta \text{Re}(\alpha) = \left(\frac{\ddot{I}_L}{\Gamma_L} + \dot{I}_L - \frac{\ddot{I}_R}{\Gamma_R} - \dot{I}_R \right) + \frac{\tilde{\Gamma}}{2} \left(\frac{\dot{I}_L}{\Gamma_L} + I_L - \frac{\dot{I}_R}{\Gamma_R} - I_R \right) + 4g_{\text{res}}^2 \left(\frac{I_L - \gamma_L^+}{\Gamma_L} - \frac{I_R - \gamma_R^+}{\Gamma_R} \right), \quad (9a)$$

$$-4 g_{\text{off}} E \text{Re}(\beta) = \left(\frac{\ddot{I}_L}{\Gamma_L} + \dot{I}_L + \frac{\ddot{I}_R}{\Gamma_R} + \dot{I}_R \right) + \frac{\tilde{\Gamma}}{2} \left(\frac{\dot{I}_L}{\Gamma_L} + I_L + \frac{\dot{I}_R}{\Gamma_R} + I_R \right) + 4g_{\text{off}}^2 \left(\frac{I_L - \gamma_L^+}{\Gamma_L} + \frac{I_R - \gamma_R^+}{\Gamma_R} + 1 \right). \quad (9b)$$

Here, $\alpha \equiv \langle 01 | \hat{\rho} | 10 \rangle$ and $\beta \equiv \langle 00 | \hat{\rho} | 11 \rangle$ are coherences (in purple in Fig. 1), $\delta = \varepsilon_L - \varepsilon_R$ is the energy detuning between the qubits, $E = \varepsilon_L + \varepsilon_R + U$ the energy of the doubly-occupied state $|11\rangle$, $\tilde{\Gamma} = \Gamma_L + \Gamma_R + 2\Gamma_z$ the total dissipation strength and $\Gamma_z = \gamma_L^z + \gamma_R^z$ the total pure dephasing strength.

The sets of equations (6), (8) and (9) constitute the main results of this work. They demonstrate the possibility to access specific complex elements of the density operator of an open quantum system through transport

quantities evaluated at a certain time. Interestingly, the set of accessible coherences depends on the evolution properties of the system, and exactly corresponds to the coherences being non-zero in the steady-state regime (see Appendix A). In Table I, we summarize the features of the transport approach to two-qubit QST for specific cases of Eq. (7). More generally, accessing all density matrix's elements is possible, but it requires a Hamiltonian involving additional operators (see Appendix B). While analytical expressions are cumbersome and

Case	Populations	Transport quantities	Transport parameters
	r_{00}, r_{01}, r_{10}	$I_L, I_R,$ S_{LR}	$\gamma_L^\pm, \gamma_R^\pm$

Case	Generated coherences	Additional transport quantities	Hamiltonian param. and add. measurements
	α, β	\dot{I}_L, \dot{I}_L and \dot{I}_R, \dot{I}_R	$g_{\text{res}}, g_{\text{off}},$ δ, E ; $I_L^{(3)}$ or $I_R^{(3)}$
$\delta = 0$ $E = 0$	$\text{Im}(\alpha), \text{Im}(\beta)$	\dot{I}_L and \dot{I}_R	$g_{\text{res}}, g_{\text{off}}$; \emptyset
$g_{\text{off}} = 0$	$\text{Im}(\alpha), \text{Re}(\alpha)$	\dot{I}_L, \dot{I}_L or \dot{I}_R, \dot{I}_R	$g_{\text{res}},$ δ ; $I_L^{(3)}$ or $I_R^{(3)}$

TABLE I. Table summarizing which transport quantities (in blue) are necessary to reconstruct the populations and coherences. The general case is defined by Eq. (7), and two variants are considered. The rightmost column lists the transport and Hamiltonian parameters (in green) which *a priori* knowledge is necessary, and the additional measurements required to determine pure dephasing. Additional transport-based quantities can be exploited to determine the Hamiltonian's parameters as well (see Appendix D).

measurements more challenging, there is no conceptual difference from the case presented here in details. In the most general case, we show in Appendix C that two-time correlation functions $S_{j_1 j_2}(t_1, t_2)$ could be exploited for QST despite their complexity. In contrast, auto-correlation functions evaluated at the same time $S_{jj}(t, t)$ provide the same type of information as average currents, *i.e.* information about the populations.

Steady-state regime.— This transport approach to QST is particularly advantageous in the steady state (*ss*), where all current time-derivatives vanish. Then, the populations and coherences are simply accessed by the measurements of the steady-state currents and noise, see Appendix E for general expressions. In the case of a zero off-resonant inter-qubit interaction ($g_{\text{off}} = 0$), of specific

interest in the context of entanglement generation from out-of-equilibrium currents [29, 33], current conservation implies $I_L^{ss} = -I_R^{ss} \equiv I^{ss}$ and only the α -coherence remains finite. Its real and imaginary parts can be reconstructed with

$$2g_{\text{res}}\text{Im}(\alpha)^{ss} = -I^{ss}, \quad (10a)$$

$$2g_{\text{res}}\delta\text{Re}(\alpha)^{ss} = 2g_{\text{res}}^2 \left(\frac{\gamma_L^+}{\Gamma_L} - \frac{\gamma_R^+}{\Gamma_R} \right) - \left(\frac{\tilde{\Gamma}}{2} + \frac{4g_{\text{res}}^2}{\Gamma_L \Gamma_R} \frac{\Gamma}{2} \right) I^{ss}. \quad (10b)$$

Interestingly, the first equation corresponds to previously-established connection between steady-state currents and non-zero coherences in this setup. While it was derived analytically in the steady-state regime in previous works [33, 35, 41], this work provides a complete and fundamental reason for this connection (see Appendix F). Additionally, the measurement of the steady-state current averages and correlations allows us to determine the pure dephasing strength $\Gamma_z = \tilde{\Gamma} - \Gamma$ if the other dynamics parameters are known. Indeed, taking the time derivative of Eq. (9b) and its steady-state limit yields (see Appendix D)

$$\left(\left(\frac{\tilde{\Gamma}}{2} \right)^2 + \frac{g_{\text{res}}^2 \Gamma \tilde{\Gamma}}{\Gamma_L \Gamma_R} + \delta^2 \right) I^{ss} = 2g_{\text{res}}^2 \tilde{\Gamma} \left(\frac{\gamma_L^+}{\Gamma_L} - \frac{\gamma_R^+}{\Gamma_R} \right), \quad (11)$$

from which $\tilde{\Gamma}$ can be extracted.

Transport-based entanglement witness.— Remarkably, our demonstration of complete transport-based QST allows us to express entanglement witnesses in terms of currents and associated quantities only. While the concurrence is defined from the Schmidt coefficients [42], it takes a particular simple form for X-shaped density matrices [43]: $\mathcal{C} = 2 \max\{0, |\alpha| - \sqrt{r_{00}r_{11}}, |\beta| - \sqrt{r_{01}r_{10}}\}$. In the illustrative case of two energy-degenerate qubits ($\delta = 0$) with resonant interaction only ($g_{\text{off}} = 0$), initialized in their ground state, the density matrix $\rho(t)$ remains X-shaped at all time t and its concurrence can then be expressed as:

$$\mathcal{C} = \max \left\{ 0, \left| \frac{1}{g_{\text{res}}} \left(\frac{\dot{I}_L}{\Gamma_L} + I_L \right) \right| - 2 \sqrt{\left(\frac{S_{LR}}{\Gamma_L \Gamma_R} + \frac{I_L - \gamma_L^+}{\Gamma_L} \frac{I_R - \gamma_R^+}{\Gamma_R} \right) \left(\frac{S_{LR}}{\Gamma_L \Gamma_R} + \frac{I_L + \gamma_L^-}{\Gamma_L} \frac{I_R + \gamma_R^-}{\Gamma_R} \right)} \right\}. \quad (12)$$

Equation (12) shows that certifying the presence of entanglement in an open quantum system does not require QST through decoupling the system from its environments and performing projective measurements. In Appendix G, we provide the expression of \mathcal{C} in the general

case. These results formally connect entanglement measures of a quantum system and transport quantities accessible in an open device configuration.

Experimental relevance and conclusion.— Transport-based QST relies on minimal, but necessary knowledge

of the system dynamics and system-bath coupling strengths. Precisely, measuring the latter corresponds to state-of-the-art knowledge through spectroscopy measurements in solid-state platforms [44–47]. As for the former and the potential presence of dephasing, recent experiments on hybrid setups have demonstrated the possibility to estimate them. As an alternative, we show in Appendix D that additional transport quantities, current derivatives measured at different times, do provide this information. Therefore, such necessary knowledge does not constitute a limitation to the applicability of our proposal. This work is a significant step towards demonstrating complete QST

from measuring out-of-equilibrium environments and induced transport properties. It treats the specific case of two qubits embedded into a two-terminal device. Open questions for future works concern in particular its generalization to an arbitrary d-dimension open quantum system, error mitigation to be investigated in this context [48], and its experimental demonstration, for instance in solid-state platforms.

Acknowledgements.— We are thankful for fruitful discussions with Landry Bretheau and Gwendal Fève, and useful feedbacks from Vincenzo Savona. All authors acknowledge the support of NCCR SwissMAP.

-
- [1] *Quantum State Estimation* (Springer Berlin Heidelberg, 2004).
- [2] M. A. Nielsen and I. L. Chuang, *Quantum Computation and Quantum Information: 10th Anniversary Edition* (Cambridge University Press, 2012).
- [3] K. Vogel and H. Risken, *Physical Review A* **40**, 2847–2849 (1989).
- [4] S. Filipp, P. Maurer, P. J. Leek, M. Baur, R. Bianchetti, J. M. Fink, M. Göppl, L. Steffen, J. M. Gambetta, A. Blais, and A. Wallraff, *Physical Review Letters* **102** (2009), 10.1103/physrevlett.102.200402.
- [5] R. Bianchetti, S. Filipp, M. Baur, J. M. Fink, C. Lang, L. Steffen, M. Boissonneault, A. Blais, and A. Wallraff, *Physical Review Letters* **105** (2010), 10.1103/physrevlett.105.223601.
- [6] C. F. Roos, G. P. T. Lancaster, M. Riebe, H. Häffner, W. Hänsel, S. Gulde, C. Becher, J. Eschner, F. Schmidt-Kaler, and R. Blatt, *Physical Review Letters* **92** (2004), 10.1103/physrevlett.92.220402.
- [7] H. Häffner, W. Hänsel, C. F. Roos, J. Benhelm, D. Chekhal kar, M. Chwalla, T. Körber, U. D. Rapol, M. Riebe, P. O. Schmidt, C. Becher, O. Gühne, W. Dür, and R. Blatt, *Nature* **438**, 643–646 (2005).
- [8] G. M. Leskowitz and L. J. Mueller, *Physical Review A* **69** (2004), 10.1103/physreva.69.052302.
- [9] J. Wrachtrup and F. Jelezko, *Journal of Physics: Condensed Matter* **18**, S807–S824 (2006).
- [10] D. F. V. James, P. G. Kwiat, W. J. Munro, and A. G. White, *Physical Review A* **64** (2001), 10.1103/physreva.64.052312.
- [11] K. Bartkiewicz, A. Černoč, K. Lemr, and A. Miranowicz, *Scientific Reports* **6** (2016), 10.1038/srep19610.
- [12] H.-Y. Huang, R. Kueng, and J. Preskill, *Nature Physics* **16**, 1050–1057 (2020).
- [13] K. Thapliyal, S. Banerjee, and A. Pathak, *Annals of Physics* **366**, 148–167 (2016).
- [14] P. Kurpiers, P. Magnard, T. Walter, B. Royer, M. Pechal, J. Heinsoo, Y. Salathé, A. Akin, S. Storz, J.-C. Besse, S. Gasparinetti, A. Blais, and A. Wallraff, *Nature* **558**, 264–267 (2018).
- [15] S. Storz, J. Schär, A. Kulikov, P. Magnard, P. Kurpiers, J. Lütolf, T. Walter, A. Copetudo, K. Reuer, A. Akin, J.-C. Besse, M. Gabureac, G. J. Norris, A. Rosario, F. Martin, J. Martinez, W. Amaya, M. W. Mitchell, C. Abellan, J.-D. Bancal, N. Sangouard, B. Royer, A. Blais, and A. Wallraff, *Nature* **617**, 265–270 (2023).
- [16] G. Torlai, G. Mazzola, J. Carrasquilla, M. Troyer, R. Melko, and G. Carleo, *Nature Physics* **14**, 447–450 (2018).
- [17] D. A. Lidar, I. L. Chuang, and K. B. Whaley, *Physical Review Letters* **81**, 2594–2597 (1998).
- [18] P. G. Kwiat, A. J. Berglund, J. B. Altepeter, and A. G. White, *Science* **290**, 498–501 (2000).
- [19] D. Kielpinski, V. Meyer, M. A. Rowe, C. A. Sackett, W. M. Itano, C. Monroe, and D. J. Wineland, *Science* **291**, 1013–1015 (2001).
- [20] D. Kielpinski, C. Monroe, and D. J. Wineland, *Nature* **417**, 709–711 (2002).
- [21] Z. J. Deng, M. Feng, and K. L. Gao, *Physical Review A* **75** (2007), 10.1103/physreva.75.024302.
- [22] F. Reiter, A. S. Sørensen, P. Zoller, and C. A. Muschik, *Nature Communications* **8** (2017), 10.1038/s41467-017-01895-5.
- [23] Q. Xu, G. Zheng, Y.-X. Wang, P. Zoller, A. A. Clerk, and L. Jiang, *npj Quantum Information* **9** (2023), 10.1038/s41534-023-00746-0.
- [24] T. Hillmann and F. Quijandria, *Physical Review A* **107** (2023), 10.1103/physreva.107.032423.
- [25] V. Eisler and Z. Zimborás, *Physical Review A* **71** (2005), 10.1103/physreva.71.042318.
- [26] L. Hartmann, W. Dür, and H. J. Briegel, *New Journal of Physics* **9**, 230–230 (2007).
- [27] L. Quiroga, F. J. Rodríguez, M. E. Ramírez, and R. París, *Physical Review A* **75** (2007), 10.1103/physreva.75.032308.
- [28] B. Bellomo and M. Antezza, *New Journal of Physics* **15**, 113052 (2013).
- [29] J. Bohr Brask, G. Haack, N. Brunner, and M. Huber, *New Journal of Physics* **17**, 113029 (2015).
- [30] A. Hewgill, A. Ferraro, and G. De Chiara, *Physical Review A* **98** (2018), 10.1103/physreva.98.042102.
- [31] A. Das, A. A. Khan, S. D. Mishra, P. Solanki, B. De, B. Muralidharan, and S. Vinjanampathy, *Quantum Science and Technology* **7**, 045034 (2022).
- [32] S. Khandelwal, B. Annby-Andersson, G. F. Diotallevi, A. Wacker, and A. Tavakoli, “Maximal steady-state entanglement in autonomous quantum thermal machines,” (2024).
- [33] S. Khandelwal, N. Palazzo, N. Brunner, and G. Haack, *New Journal of Physics* **22**, 073039 (2020).

- [34] D. Farina, B. Benazout, F. Centrone, and A. Acin, “Thermodynamic precision in the nonequilibrium exchange scenario,” (2023).
- [35] G. Francesco Diotallevi, B. Annby-Andersson, P. Samuelsson, A. Tavakoli, and P. Bakhshinezhad, *New Journal of Physics* **26**, 053005 (2024).
- [36] H.-P. Breuer and F. Petruccione, *The Theory of Open Quantum Systems* (Oxford University Press/Oxford, 2007).
- [37] G. Schaller, “Dynamics of open quantum systems,” in *Open Quantum Systems Far from Equilibrium* (Springer International Publishing, 2014) p. 1–26.
- [38] P. P. Hofer, M. Perarnau-Llobet, L. D. M. Miranda, G. Haack, R. Silva, J. B. Brask, and N. Brunner, *New Journal of Physics* **19**, 123037 (2017).
- [39] G. T. Landi, M. J. Kewming, M. T. Mitchison, and P. P. Potts, *PRX Quantum* **5** (2024), 10.1103/prxquantum.5.020201.
- [40] G. Blasi, S. Khandelwal, and G. Haack, *Physical Review Research* **6** (2024), 10.1103/physrevresearch.6.043091.
- [41] J. Bourgeois, G. Blasi, S. Khandelwal, and G. Haack, *Entropy* **26**, 497 (2024).
- [42] W. K. Wootters, *Physical Review Letters* **80**, 2245–2248 (1998).
- [43] T. Yu and J. Eberly, *Quantum Information and Computation* **7**, 459–468 (2007).
- [44] Y.-Y. Liu, K. Petersson, J. Stehlik, J. Taylor, and J. Petta, *Physical Review Letters* **113** (2014), 10.1103/physrevlett.113.036801.
- [45] A. Stockklauser, P. Scarlino, J. Koski, S. Gasparinetti, C. Andersen, C. Reichl, W. Wegscheider, T. Ihn, K. Ensslin, and A. Wallraff, *Physical Review X* **7** (2017), 10.1103/physrevx.7.011030.
- [46] Y. Wang, Y. Chen, H. T. Bui, C. Wolf, M. Haze, C. Mier, J. Kim, D.-J. Choi, C. P. Lutz, Y. Bae, S.-h. Phark, and A. J. Heinrich, *Science* **382**, 87–92 (2023).
- [47] H. Duprez, S. Cances, A. Omahen, M. Masseroni, M. J. Ruckriegel, C. Adam, C. Tong, R. Garreis, J. D. Gerber, W. Huang, L. Gächter, K. Watanabe, T. Taniguchi, T. Ihn, and K. Ensslin, *Nature Communications* **15** (2024), 10.1038/s41467-024-54121-4.
- [48] M. Cramer, M. B. Plenio, S. T. Flammia, R. Somma, D. Gross, S. D. Bartlett, O. Landon-Cardinal, D. Poulin, and Y.-K. Liu, *Nature Communications* **1** (2010), 10.1038/ncomms1147.
- [49] M. Cattaneo, G. L. Giorgi, S. Maniscalco, and R. Zambrini, *New Journal of Physics* **21**, 113045 (2019).

Appendix A: Methodology

1. Local master equation

Our model of the system's evolution is based on the local Lindblad master equation:

$$\dot{\hat{\rho}} = \mathcal{L}\hat{\rho} = -i[\hat{H}_S, \hat{\rho}] + \sum_{j=L,R} (\gamma_j^+ \mathcal{D}[\hat{\sigma}_+^{(j)}] + \gamma_j^- \mathcal{D}[\hat{\sigma}_-^{(j)}])\hat{\rho} + \sum_{j=L,R} \frac{\gamma_j^z}{2} \mathcal{D}[\hat{\sigma}_z^{(j)}]\hat{\rho}, \quad (\text{A1})$$

with $\mathcal{D}[A]\cdot \equiv A \cdot A^\dagger - \{A^\dagger A, \cdot\}/2$, $\{A, B\} = AB + BA$ and $[A, B] = AB - BA$. Denoting γ_j the bare reservoir-qubit coupling rate at side j and $n_{F/B}^j(\epsilon) = (1 \pm e^{(\epsilon - \mu_j)/T_j})^{-1}$ the distribution occupation of bath j (respectively for a fermionic or bosonic reservoir), the in- and out-going coupling rates γ_j^+ , γ_j^- are given by

$$\gamma_j^+ = \gamma_j n_{F/B}^j(\epsilon_j) \quad \text{and} \quad \gamma_j^- = \gamma_j (1 \mp n_{F/B}^j(\epsilon_j)), \quad (\text{A2})$$

with the upper sign for fermions and the lower one for bosons. Such equation correctly captures the dynamics for Markovian reservoirs, weakly coupled to the system and qubits weakly inter-connected, i.e.:

$$\gamma_L, \gamma_R \ll T_L, T_R, |\epsilon_L - \mu_L|, |\epsilon_R - \mu_R| \quad \text{and} \quad g_{\text{res}}, g_{\text{off}} \lesssim \gamma_j. \quad (\text{A3})$$

If the assumption of weak inter-qubit coupling is not satisfied, the global Master equation provides a more accurate description of the system's evolution, see for instance [49]. While the equations for currents and noise will be different, there is no conceptual difference with the case treated in this work.

2. Vectorization of the open quantum system

To compute the results presented in the main text, we perform a vectorization of the density matrix, following the convention

$$|n_L n_R\rangle \langle m_L m_R| \longrightarrow |n_L n_R\rangle \otimes |m_L m_R\rangle. \quad (\text{A4})$$

Into such representation, superoperators transform into operators as

$$\mathcal{A} = \hat{A}_1 \cdot \hat{A}_2 \longrightarrow \mathbf{A} = (\hat{A}_1 \otimes \hat{A}_2^T). \quad (\text{A5})$$

Hereafter, we move to the basis where the density matrix

$$\rho = \begin{pmatrix} r_{00} & v & x & \beta \\ v^* & r_{01} & \alpha & y \\ x^* & \alpha^* & r_{10} & z \\ \beta^* & y^* & z^* & r_{11} \end{pmatrix} \quad (\text{A6})$$

is described by the vector

$$\vec{\rho} = (r_{00}, r_{01}, r_{10}, r_{11}, \text{Im}(\alpha), \text{Re}(\alpha), \text{Im}(\beta), \text{Re}(\beta), \text{Im}(x), \text{Re}(x), \text{Im}(y), \text{Re}(y), \text{Im}(v), \text{Re}(v), \text{Im}(z), \text{Re}(z))^T. \quad (\text{A7})$$

3. Structure of the Lindbladian

Following this vectorization, the evolution equation (1) resumes to a linear differential equation:

$$\partial_t \vec{\rho}(t) = \mathbf{L} \vec{\rho}(t) \quad (\text{A8})$$

with the Lindblad matrix $\mathbf{L} = \mathbf{L}_{\text{unit}} + \mathbf{L}_{\text{diss}}$ made of two components:

$$\mathbf{L}_{\text{unit}} = -i(H_S \otimes \mathbb{I}_4 - \mathbb{I}_4 \otimes H_S^T) \quad (\text{A9})$$

describing the unitary evolution, and

$$\mathbf{L}_{\text{diss}} = \sum_{j=L,R} (\mathbf{L}_j^+ + \mathbf{L}_j^- + \mathbf{L}_j^z), \quad \text{where } \mathbf{L}_j^\alpha = \gamma_j^\alpha (\sigma_\alpha^{(j)} \otimes \sigma_\alpha^{(j)} - \frac{1}{2} (\sigma_\alpha^{(j)\dagger} \sigma_\alpha^{(j)} \otimes \mathbb{I}_4 + \mathbb{I}_4 \otimes (\sigma_\alpha^{(j)\dagger} \sigma_\alpha^{(j)})^T), \quad (\text{A10})$$

the dissipative evolution. The matrices \mathbf{L}_{unit} and \mathbf{L}_{diss} may be decomposed into 16 blocks of dimension 4×4 , corresponding to the different components of the dynamics:

- i) The evolution set by the dissipative terms, induced by the presence of reservoirs and of pure dephasing, is captured by the block-diagonal matrix

$$\mathbf{L}_{\text{diss}} = \begin{pmatrix} \boxed{\mathbf{L}_{\text{pop}}} & & & \\ & \boxed{\mathbf{L}_{\alpha,\beta}} & & \\ & & \boxed{\mathbf{L}_{x,y}} & \\ & & & \boxed{\mathbf{L}_{v,z}} \end{pmatrix} \quad (\text{A11})$$

with

$$\mathbf{L}_{\text{pop}} = \begin{pmatrix} -(\gamma_L^+ + \gamma_R^+) & \gamma_R^- & \gamma_L^- & 0 \\ \gamma_R^+ & -(\gamma_L^+ + \gamma_R^-) & 0 & \gamma_L^- \\ \gamma_L^+ & 0 & -(\gamma_L^- + \gamma_R^+) & \gamma_R^- \\ 0 & \gamma_L^+ & \gamma_R^+ & -(\gamma_L^- + \gamma_R^-) \end{pmatrix}, \quad (\text{A12})$$

$$\mathbf{L}_{\alpha,\beta} = -\frac{\tilde{\Gamma}}{2} \mathbb{I}_4, \quad (\text{A13})$$

$$\mathbf{L}_{x,y} = -\frac{\Gamma_L + 2\gamma_L^z}{2} \mathbb{I}_4 + \begin{pmatrix} -\gamma_R^+ & 0 & \gamma_R^- & 0 \\ 0 & -\gamma_R^+ & 0 & \gamma_R^- \\ \gamma_R^+ & 0 & -\gamma_R^- & 0 \\ 0 & \gamma_R^+ & 0 & -\gamma_R^- \end{pmatrix}, \quad (\text{A14})$$

$$\mathbf{L}_{v,z} = -\frac{\Gamma_R + 2\gamma_R^z}{2} \mathbb{I}_4 + \begin{pmatrix} -\gamma_L^+ & 0 & \gamma_L^- & 0 \\ 0 & -\gamma_L^+ & 0 & \gamma_L^- \\ \gamma_L^+ & 0 & -\gamma_L^- & 0 \\ 0 & \gamma_L^+ & 0 & -\gamma_L^- \end{pmatrix}. \quad (\text{A15})$$

It exponentially suppresses the coherences, as expected, while generating coupling between the populations and between pairs of coherences, (x, y) and (v, z) .

- ii) On-site energies and interaction, $H_{\text{on-site}} = \epsilon_L \hat{n}_L + \epsilon_R \hat{n}_R + U \hat{n}_L \hat{n}_R$, yields a superoperator which is also block diagonal in this basis, with

$$\mathbb{L}_{\text{on-site}} = \begin{pmatrix} \boxed{\begin{matrix} 0 \\ 0 \\ 0 \\ 0 \end{matrix}} & & & \\ & \boxed{\begin{matrix} 0 & \delta \\ -\delta & 0 \\ 0 & E \\ -E & 0 \end{matrix}} & & \\ & & \boxed{\begin{matrix} 0 & \epsilon_L \\ -\epsilon_L & 0 \\ 0 & \epsilon_L + U \\ -(\epsilon_L + U) & 0 \end{matrix}} & \\ & & & \boxed{\begin{matrix} 0 & \epsilon_R \\ -\epsilon_R & 0 \\ 0 & \epsilon_R + U \\ -(\epsilon_R + U) & 0 \end{matrix}} \end{pmatrix}. \quad (\text{A16})$$

It couples real and imaginary parts of the coherences.

- iii) Interaction between the two qubits, $H_{\text{int}} = g_{\text{res}} (\hat{\sigma}_+^{(L)} \hat{\sigma}_-^{(R)} + \hat{\sigma}_-^{(L)} \hat{\sigma}_+^{(R)}) + g_{\text{off}} (\hat{\sigma}_+^{(L)} \hat{\sigma}_+^{(R)} + \hat{\sigma}_-^{(L)} \hat{\sigma}_-^{(R)})$, reads:

$$\mathbb{L}_{\text{int}} = \begin{pmatrix} \boxed{} & -2\mathbf{L}_{\text{int}}^{(1)T} & & \\ \mathbf{L}_{\text{int}}^{(1)} & \boxed{} & & \\ & & \boxed{} & -\mathbf{L}_{\text{int}}^{(2)T} \\ & & \mathbf{L}_{\text{int}}^{(2)} & \boxed{} \end{pmatrix} \quad (\text{A17})$$

with

$$\mathbf{L}_{\text{int}}^{(1)} = \begin{pmatrix} 0 & g_{\text{res}} & -g_{\text{res}} & 0 \\ 0 & 0 & 0 & 0 \\ 0 & 0 & 0 & 0 \\ 0 & 0 & 0 & 0 \end{pmatrix} + \begin{pmatrix} 0 & 0 & 0 & 0 \\ 0 & 0 & 0 & 0 \\ g_{\text{off}} & 0 & 0 & -g_{\text{off}} \\ 0 & 0 & 0 & 0 \end{pmatrix}, \quad (\text{A18})$$

$$\mathbf{L}_{\text{int}}^{(2)} = \begin{pmatrix} 0 & g_{\text{res}} & 0 & 0 \\ -g_{\text{res}} & 0 & 0 & 0 \\ 0 & 0 & -g_{\text{res}} & 0 \\ 0 & 0 & g_{\text{res}} & 0 \end{pmatrix} + \begin{pmatrix} 0 & 0 & 0 & -g_{\text{off}} \\ 0 & 0 & -g_{\text{off}} & 0 \\ 0 & g_{\text{off}} & 0 & 0 \\ g_{\text{off}} & 0 & 0 & 0 \end{pmatrix}. \quad (\text{A19})$$

The resonant part of the inter-qubit interaction couples the populations and the α -coherence's dynamics, while the off-resonant part couples the populations and the β -coherence's dynamics. They also interconnect the (x, y) and (v, z) pairs of coherences.

4. Transport approach to QST

The current averages, given by Eq. (4), and their time-derivatives may be expressed as

$$I_j(t) = \gamma_j^+ - \Gamma_j \vec{n}_j \cdot \vec{\rho}(t), \quad \dot{I}_j^{(k)}(t) = -\Gamma_j (\mathbb{L}^T)^k \vec{n}_j \cdot \vec{\rho}(t) \quad (\text{A20})$$

with $\vec{n}_L = (0, 0, 1, 1, 0, \dots, 0)^T$, $\vec{n}_R = (0, 1, 0, 1, 0, \dots, 0)^T$ and \cdot representing the scalar product. Measuring current averages and their time-derivatives is thus equivalent to applying some operators $\vec{n}_j^T \mathbb{L}^k$ on the vector $\vec{\rho}$. For $k = 0$, this corresponds to measuring the populations of the quantum state. For $k = 1$, it involves the coherences that are directly coupled to the population set. If they are up to two, measuring $(I_L(t), I_R(t), \dot{I}_L(t), \dot{I}_R(t))$ is enough to determine them. For $k \geq 2$, we recover coherences that are indirectly coupled to the populations. Overall, our transport-based QST protocol provides a complete tomography for density matrices lying in the subspace

$$\mathcal{V} := \text{span}\{(\mathbb{L}^T)^k \vec{n}_j, j = L, R, k \geq 0\} \quad (\text{A21})$$

of the two-qubit system's Hilbert space, i.e. density matrices whose finite coherences have a coupled evolution with the populations. Note that these coherences are of major experimental relevance, as they are the only ones that are generated from finite populations, and the only ones that survive dissipation in the steady-state.

Appendix B: Generalization towards complete QST

To perform complete QST of a full density matrix, one needs to consider a Hamiltonian with additional elements - for example, local drives on the qubits, $H_{\text{drive}} := f_L(\sigma_+^{(L)} + \sigma_-^{(L)}) + f_R(\sigma_+^{(R)} + \sigma_-^{(R)})$ with f_L and f_R real amplitudes of the drives. The matrix of the associated superoperator, decomposed into 4×4 blocks, reads:

$$\mathbf{L}_{\text{drive}} = \left(\begin{array}{c|c|c|c} \boxed{} & & & \\ \hline \boxed{} & & & \\ \hline \mathbf{L}_{\text{drive}}^{(L1)} & & & \\ \hline \boxed{} & & & \\ \hline \mathbf{L}_{\text{int}}^{(L2)} & & & \\ \hline \boxed{} & & & \\ \hline \end{array} \begin{array}{c} -2\mathbf{L}_{\text{drive}}^{(L1)T} \\ \\ \\ \\ \\ \\ \\ \end{array} \begin{array}{c|c|c|c} \boxed{} & & & \\ \hline \boxed{} & & & \\ \hline \mathbf{L}_{\text{drive}}^{(L2)T} & & & \\ \hline \boxed{} & & & \\ \hline \mathbf{L}_{\text{int}}^{(L2)} & & & \\ \hline \boxed{} & & & \\ \hline \end{array} \right) + \left(\begin{array}{c|c|c|c} \boxed{} & & & \\ \hline \boxed{} & & & \\ \hline \mathbf{L}_{\text{drive}}^{(R1)} & & & \\ \hline \boxed{} & & & \\ \hline \mathbf{L}_{\text{int}}^{(R2)} & & & \\ \hline \boxed{} & & & \\ \hline \end{array} \begin{array}{c} -2\mathbf{L}_{\text{drive}}^{(R1)T} \\ \\ \\ \\ \\ \\ \\ \end{array} \begin{array}{c|c|c|c} \boxed{} & & & \\ \hline \boxed{} & & & \\ \hline \mathbf{L}_{\text{drive}}^{(R2)T} & & & \\ \hline \boxed{} & & & \\ \hline \mathbf{L}_{\text{int}}^{(R2)} & & & \\ \hline \boxed{} & & & \\ \hline \end{array} \right) \quad (\text{B1})$$

with

$$\mathbf{L}_{\text{int}}^{(L1)} = \begin{pmatrix} f_L & 0 & -f_L & 0 \\ 0 & 0 & 0 & 0 \\ 0 & f_L & 0 & -f_L \\ 0 & 0 & 0 & 0 \end{pmatrix}, \quad \mathbf{L}_{\text{int}}^{(L2)} = \begin{pmatrix} 0 & -f_L & 0 & f_L \\ -f_L & 0 & -f_L & 0 \\ 0 & f_L & 0 & -f_L \\ f_L & 0 & f_L & 0 \end{pmatrix}, \quad (\text{B2})$$

$$\mathbf{L}_{\text{int}}^{(R1)} = \begin{pmatrix} f_R & -f_R & 0 & 0 \\ 0 & 0 & 0 & 0 \\ 0 & 0 & f_R & -f_R \\ 0 & 0 & 0 & 0 \end{pmatrix}, \quad \mathbf{L}_{\text{int}}^{(R2)} = \begin{pmatrix} 0 & -f_R & 0 & f_R \\ f_R & 0 & -f_R & 0 \\ 0 & f_R & 0 & -f_R \\ -f_R & 0 & f_R & 0 \end{pmatrix}. \quad (\text{B3})$$

The drive on qubit L (respectively on qubit R) couples the evolution of the populations and with the one of the (x, y) (resp. (v, z)) coherence pair of coherences, and of (α, β) and (v, z) (resp. (x, y)).

The total Hamiltonian $H_{\text{tot}} = H_{\text{on-site}} + H_{\text{int}} + H_{\text{drive}}$ is a full matrix, with

$$H_{\text{tot}} = \begin{pmatrix} 0 & f_R & f_L & g_{\text{off}} \\ f_R & \epsilon_R & g_{\text{res}} & f_L \\ f_L & g_{\text{res}} & \epsilon_R & f_R \\ g_{\text{off}} & f_L & f_R & E \end{pmatrix}. \quad (\text{B4})$$

In this case, all coherences are generated. Eq. (8) generalizes to:

$$\frac{\dot{I}_L(t)}{\Gamma_L} + I_L(t) = -2g_{\text{off}}\text{Im}(\beta)(t) - g_{\text{res}}\text{Im}(\alpha)(t) - f_L\text{Im}(x(t) + y(t)), \quad (\text{B5})$$

$$\frac{\dot{I}_R(t)}{\Gamma_R} + I_R(t) = -2g_{\text{off}}\text{Im}(\beta)(t) + g_{\text{res}}\text{Im}(\alpha)(t) - f_L\text{Im}(v(t) + z(t)). \quad (\text{B6})$$

The imaginary part of the α and β coherences cannot be determined from $(\dot{I}_L, I_L, \dot{I}_R, I_R)$ anymore. To get a closed set of equations on the coherences, one needs to consider additional equations, obtained similarly from higher derivatives.

Appendix C: Current correlation functions

1. Definitions

The quantum jumps of excitations tunneling into (respectively out of) the system, induced by the presence of reservoir j , are described within the local Lindblad master equation formalism by the superoperators

$$\mathcal{L}_j^+ := \gamma_j^+ \sigma_+^{(j)} \cdot \sigma_-^{(j)}, \quad (\text{C1})$$

$$\mathcal{L}_j^- := \gamma_j^- \sigma_-^{(j)} \cdot \sigma_+^{(j)}. \quad (\text{C2})$$

It was recently derived in [40], using a full-counting statistics approach, that within this formalism, the correlation function $S_{j_1 j_2}(t_1, t_2)$ between the currents in reservoir j_1 at time t_1 and j_2 at time t_2 equals to

$$\begin{aligned} S_{j_1 j_2}(t_1, t_2) &:= \delta_{j_1, j_2} \delta(t_1 - t_2) \text{Tr}\{\mathcal{A}_{j_1} \hat{\rho}(t_1)\} \\ &+ \Theta(t_1 - t_2) \text{Tr}\left\{\mathcal{I}_{j_1} e^{\mathcal{L}(t_1 - t_2)} \mathcal{I}_{j_2} \hat{\rho}(t_2)\right\} \\ &+ \Theta(t_2 - t_1) \text{Tr}\left\{\mathcal{I}_{j_2} e^{\mathcal{L}(t_2 - t_1)} \mathcal{I}_{j_1} \hat{\rho}(t_1)\right\} \\ &- \text{Tr}\{\mathcal{I}_{j_1} \hat{\rho}(t_1)\} \text{Tr}\{\mathcal{I}_{j_2} \hat{\rho}(t_2)\}, \end{aligned} \quad (\text{C3})$$

with $\mathcal{I}_j := \mathcal{L}_j^+ - \mathcal{L}_j^-$ and $\mathcal{A}_j := \mathcal{L}_j^+ + \mathcal{L}_j^-$ the current and activity superoperators associated to reservoir j . The first term of this expression, the dynamical activity $A_{j_1}(t) = \text{Tr}[\mathcal{A}_{j_1} \hat{\rho}(t)]$, is present only for instantaneous auto-correlation functions and describes the rate of jumps occurring at the interface with the reservoir j , regardless of their direction.

2. Instantaneous auto-correlation functions

The instantaneous ($t_1 = t_2 = t$) auto-correlation functions are formally given by:

$$S_{j,j}(t, t) = \delta(0)A_j(t) + \text{Tr}[\mathcal{I}_j^2 \hat{\rho}(t)] - I_j(t)^2. \quad (\text{C4})$$

The presence of the δ -distribution in this definition calls for a special care when manipulating $S_{j,j}(t, t)$. This is usually done by working in the frequency domain, analyzing measurements performed over a time window rather than at a fixed time. As for the transport-based QST, we note that the instantaneous auto-correlation functions do not provide further information on the quantum state than the current averages, since

$$\text{Tr}[\mathcal{I}_j^2 \hat{\rho}(t)] - I_j(t)^2 = -\Gamma_j(\gamma_j^+(1 - n_j(t))^2 + \gamma_j^- n_j(t)^2), \quad (\text{C5})$$

$$A_j(t) = \gamma_j^+(1 - n_j(t)) + \gamma_j^- n_j(t). \quad (\text{C6})$$

For this reason, we believe the instantaneous auto-correlation functions would not be relevant for transport-based QST.

3. Two-time correlation functions

In general, the superoperator $e^{\mathcal{L}(t_1-t_2)}$ corresponds to very complex matrix, whose analytical expression is not to be given here. Still, one may explore the information contained in the two-time correlation functions by studying the matrices

$$\mathcal{I}_L \rho(t) = \begin{pmatrix} -\gamma_L^- r_{10}(t) & -\gamma_L^- z(t) & 0 & 0 \\ -\gamma_L^- z^*(t) & -\gamma_L^- r_{11}(t) & 0 & 0 \\ 0 & 0 & \gamma_L^+ r_{00}(t) & \gamma_L^+ v(t) \\ 0 & 0 & \gamma_L^+ v^*(t) & \gamma_L^+ r_{01}(t) \end{pmatrix}$$

$$\mathcal{I}_R \rho(t) = \begin{pmatrix} -\gamma_R^- r_{01}(t) & 0 & -\gamma_R^- y(t) & 0 \\ 0 & \gamma_R^+ r_{00}(t) & 0 & \gamma_R^+ x(t) \\ -\gamma_R^- y^*(t) & 0 & -\gamma_R^+ r_{11}(t) & 0 \\ 0 & \gamma_R^+ x^*(t) & 0 & \gamma_R^+ r_{10}(t) \end{pmatrix}$$

where r_{ij} , v , x , y and z are elements of the density matrix ρ , as introduced in Section A.

Importantly, the coherences $\alpha(t)$ and $\beta(t)$ are absent from these matrices, yielding that no information about these coherences can be obtained from $S_{j_1 j_2}(t_1, t_2)$ itself. This aspect justifies the need for other transport quantities, like current-average time-derivatives, to perform complete transport-based QST.

Alternatively to high-order time derivatives of the current averages, one may make use of the first time-derivatives of the instantaneous correlation functions. These new transport quantities would reduce the maximal order of current time-derivatives required to obtain a close set of equations, see Section B. For illustration, the first partial derivative of the cross-correlation function $S_{LR}(t_1, t_2)$ in t_2 , for $t_1 = t$ and $t_2 \gtrsim t$, is equal to

$$\frac{\partial S_{LR}}{\partial t_2}(t, t^+) = \text{Tr}[\mathcal{I}_R \mathcal{L}_{\text{tot}} \mathcal{I}_L \hat{\rho}(t)] - I_L(t) \dot{I}_R(t) \quad (\text{C7})$$

with $\mathcal{L}_{\text{tot}} = \mathcal{L}_{\text{on-site}} + \mathcal{L}_{\text{int}} + \mathcal{L}_{\text{drive}} + \mathcal{L}_{\text{diss}}$ and

$$\text{Tr}[\mathcal{I}_R \mathcal{L}_{\text{tot}} \mathcal{I}_L \hat{\rho}(t)] = -\Gamma_R \left(2f_R(\gamma_L^+ \text{Im}(v) - \gamma_L^- \text{Im}(z)) + (S_{LR}(t) + I_L(t)I_R(t)) \right). \quad (\text{C8})$$

Still, coherences without any coupled dynamics with the populations remain inaccessible to the transport-based QST.

Appendix D: How to access the system's parameters

1. Main result

The QST protocol introduced in this work relies on the precise knowledge of the system dynamics parameters. If the system's Hamiltonian \hat{H}_S or the pure dephasing strength Γ_z is not known quantitatively, it is first necessary to measure them. An extension of the transport-based QST protocol precisely allows one to estimate these dynamics parameters from additional transport observables, higher-order time derivatives of the current averages. In Table II, we summarize all necessary transport quantities to be measured to achieve such determination, depending on the completeness of H_S .

2. Formal argument

Mathematically, the evolution of our system is given by a finite linear set of differentiable equations. Accessing sufficiently high-order time derivatives of the current averages thus provides redundant information, allowing us to check the chosen parameters of the evolution equation.

More precisely, we consider the $(\mathbb{L}^k)^T \vec{n}_j$ vectors introduced in expression (A20) of the current average and their time-derivatives. Since they are \mathbb{R}^{16} -vectors, there exist $N \leq 16$ and $c_0^{(j)}, \dots, c_N^{(j)} \in \mathbb{R}$ such that $\sum_{k=0}^N c_k^{(j)} \vec{n}_j^T \mathbb{L}^k = 0$. The $c_k^{(j)}$ depend only on $j = L, R$ and the coefficients of \mathbb{L} , i.e. the evolution parameters. Then the current averages and their time-derivatives satisfy:

$$\sum_{k=0}^N c_k^{(j)} I_j^{(k)}(t) = \gamma_j^+. \quad (\text{D1})$$

Condition on H_S	Dynamics parameters	Transport quantities
	$g_{\text{res}}, g_{\text{off}},$ $\delta, E,$ Γ_z	$I_L^{(0)}(t_i), \dots, I_L^{(3)}(t_i)$ and $I_R^{(0)}(t_i), \dots, I_R^{(3)}(t_i)$ for $i = 1, \dots, 5$
$\delta = 0$ $E = 0$	$g_{\text{res}}, g_{\text{off}}$	$I_L^{(0)}(t_i), \dots, I_L^{(2)}(t_i)$ and $I_R^{(0)}(t_i), \dots, I_R^{(2)}(t_i)$ for $i = 1, 2, 3$
$g_{\text{off}} = 0$	$g_{\text{res}},$ $\delta,$ Γ_z	$I_L^{(0)}(t_i), \dots, I_L^{(3)}(t_i)$ or $I_R^{(0)}(t_i), \dots, I_R^{(3)}(t_i)$ for $i = 1, 2, 3$

TABLE II. Summary of the transport-based dynamics probing, when all Hamiltonian and pure-dephasing parameters are missing experimental data.

Measuring the $I_j^{(k)}$ at different times provides information on the coefficient $c_k^{(j)}$, and so, on the dynamics parameters.

3. Practical implementation

In practice, the elements of the density matrix ρ may be expressed in terms of current noise $S_{LR}(t)$, average $I_j(t)$ and some of their time-derivatives $I_j^{(k)}$, so that higher current average's time-derivatives may be expressed in terms of these transport quantities, rather than density-matrix elements. Transport measurements then reveal information on the dynamics of the system.

We illustrate the method with the simplest situation of two degenerate qubits, $\epsilon_L = \epsilon_R \equiv \epsilon$, and a resonant-only interaction, $g_{\text{off}} = 0$. In this case, the dynamics only couples the population $r_{00}, r_{01}, r_{10}, r_{11}$ to the imaginary coherence $i\text{Im}(\alpha)$, with the transport-based QST's set of equations resumed to Eq. (6) and (8a). Eq. (8b) yields the current conservation identity $\frac{\dot{I}_L}{\Gamma_L} + I_L + \frac{\dot{I}_R}{\Gamma_R} + I_R = 0$, so that the QST's required transport quantities are simply $S_{LR}(t)$, $I_L(t)$, $I_R(t)$ and $\dot{I}_L(t)$. Further deriving in time Eq. (8a) brings

$$\frac{\ddot{I}_L}{\Gamma_L} + \dot{I}_L + \frac{\tilde{\Gamma}}{2} \left(\frac{\dot{I}_L}{\Gamma_L} + I_L \right) + 2g_{\text{res}}^2 \left(\frac{I_L - \gamma_L^+}{\Gamma_L} - \frac{I_R - \gamma_R^+}{\Gamma_R} \right) = 0. \quad (\text{D2})$$

If g_{res} is known *a priori*, the additional measurement of $\ddot{I}_L(t)$ at time t provides the value of $\tilde{\Gamma}$, and thus of the pure dephasing strength Γ_z . Otherwise, measuring \ddot{I}_L , \dot{I}_L , I_L and I_R at two different times t_1, t_2 determines both g_{res} and $\tilde{\Gamma}$. For error-prone measurements, the number of probe times may be increased to improve the fidelity of this protocol.

In the more general case studied in the main text, deriving in time Eq. (9) provides the equations:

$$0 = \Delta\ddot{\varphi}(t_i) + \tilde{\Gamma} \Delta\dot{\varphi}(t_i) + \left(\frac{\tilde{\Gamma}^2}{4} + \delta^2 \right) \Delta\varphi(t_i) + 4g_{\text{res}}^2 \Delta\dot{\chi}(t_i) + 2g_{\text{res}}^2 \tilde{\Gamma} \Delta\chi(t_i), \quad (\text{D3a})$$

$$0 = \ddot{\Phi}(t_i) + \tilde{\Gamma} \dot{\Phi}(t_i) + \left(\frac{\tilde{\Gamma}^2}{4} + E^2 \right) \Phi(t_i) + 4g_{\text{off}}^2 \dot{X}(t_i) + 2g_{\text{off}}^2 \tilde{\Gamma} X(t_i), \quad (\text{D3b})$$

with

$$\begin{aligned} \Delta\varphi(t) &= \varphi_L(t) - \varphi_R(t), & \Delta\chi(t) &= \chi_L(t) - \chi_R(t), \\ \Phi(t) &= \varphi_L(t) + \varphi_R(t), & X(t) &= \chi_L(t) + \chi_R(t), \\ \varphi_j(t) &= \frac{\dot{I}_j(t)}{\Gamma_j} + I_j(t), & \chi_j(t) &= \frac{I_j(t) - \gamma_j^+}{\Gamma_j}. \end{aligned}$$

In the case of an experimental set-up where all the Hamiltonian parameters are known, measuring $\ddot{I}_j(t)$ ($j = L$ or R), in addition to $\dot{I}_j(t)$, $\dot{I}_L(t)$, $\dot{I}_R(t)$, $I_L(t)$ and $I_R(t)$, determines the pure dephasing strength $\Gamma_z = \frac{1}{2}(\tilde{\Gamma} - \Gamma)$.

Otherwise, first probing the four Hamiltonian parameters $g_{\text{res}}, g_{\text{off}}, \delta, E$ requires the measurement of $I_j^{(k)}(t_i)$ for $j = L, R$ and $k = 0, 1, 2, 3$ at, at least, four different times t_i .

Appendix E: Steady-state expressions

Transport-based QST. The transport-based QST expressions Eq. (8)-(9) simplify in the steady-state, as time-derivatives vanish:

$$-4g_{\text{res}}\text{Im}(\alpha)^{ss} = I_L^{ss} - I_R^{ss}, \quad (\text{E1a})$$

$$-4g_{\text{off}}\text{Im}(\beta)^{ss} = I_L^{ss} + I_R^{ss} \quad (\text{E1b})$$

and

$$-4g_{\text{res}}\delta\text{Re}(\alpha)^{ss} = \frac{\tilde{\Gamma}}{2}(I_L^{ss} - I_R^{ss}) + 4g_{\text{res}}^2\left(\frac{I_L^{ss} - \gamma_L^+}{\Gamma_L} - \frac{I_R^{ss} - \gamma_R^+}{\Gamma_R}\right), \quad (\text{E2a})$$

$$-4g_{\text{off}}E\text{Re}(\beta)^{ss} = \frac{\tilde{\Gamma}}{2}(I_L^{ss} + I_R^{ss}) + 4g_{\text{off}}^2\left(\frac{I_L^{ss} - \gamma_L^+}{\Gamma_L} + \frac{I_R^{ss} - \gamma_R^+}{\Gamma_R} + 1\right). \quad (\text{E2b})$$

This simplification comes with one drawback: in the steady-state regime, all dynamics parameters cannot be determined with the method presented in Appendix D. Still, supposing that all the Hamiltonian parameters are known experimental data, pure dephasing may be determined with

$$0 = \left(\frac{\tilde{\Gamma}^2}{4} + \delta^2\right)(I_L^{ss} - I_R^{ss}) + 2g_{\text{res}}^2\tilde{\Gamma}\left(\frac{I_L^{ss} - \gamma_L^+}{\Gamma_L} - \frac{I_R^{ss} - \gamma_R^+}{\Gamma_R}\right), \quad (\text{E3a})$$

$$0 = \left(\frac{\tilde{\Gamma}^2}{4} + E^2\right)(I_L^{ss} + I_R^{ss}) + 2g_{\text{off}}^2\tilde{\Gamma}\left(\frac{I_L^{ss} - \gamma_L^+}{\Gamma_L} + \frac{I_R^{ss} - \gamma_R^+}{\Gamma_R} + 1\right). \quad (\text{E3b})$$

More precisely, up to two dynamics parameters can be determined through transport measurements in the steady-state.

Appendix F: Connection with current conservation laws

1. Intra-system transport quantities

The tomography technique proposed in this work can be understood as a set of transport identities by introducing new transport quantities, internal to the bipartite system.

The Hamiltonian part $H_{\text{res}} = g_{\text{res}}(\sigma_+^{(L)}\sigma_-^{(R)} + \sigma_-^{(L)}\sigma_+^{(R)})$ preserves the total number of particle in the bipartite system,

$$\text{Tr}([\hat{n}_L + \hat{n}_R, H_{\text{res}}]\hat{\rho}) = 0. \quad (\text{F1})$$

Its action generates particle transfers between the two qubits, inducing a current from the left to the right party equal by definition to

$$I_S := i \text{Tr}([\hat{n}_L, H_{\text{res}}]\hat{\rho}) = -i \text{Tr}([\hat{n}_R, H_{\text{res}}]\hat{\rho}). \quad (\text{F2})$$

For any generic density matrix, this internal current is determined by the α -coherence as

$$I_S = -2g_{\text{res}}\text{Im}(\alpha). \quad (\text{F3})$$

Meanwhile, the Hamiltonian term $H_{\text{off}} = g_{\text{off}}(\sigma_+^{(L)}\sigma_+^{(R)} + \sigma_-^{(L)}\sigma_-^{(R)})$ preserves the particle imbalance between the two parties,

$$\text{Tr}([\hat{n}_L - \hat{n}_R, H_{\text{off}}]\hat{\rho}) = 0. \quad (\text{F4})$$

Its action corresponds to a common particle production in the two qubits, given by

$$P_S := -i \text{Tr}([\hat{n}_L, H_{\text{off}}]\hat{\rho}) = -i \text{Tr}([\hat{n}_R, H_{\text{off}}]\hat{\rho}). \quad (\text{F5})$$

For any generic density matrix, this internal current is determined by the β -coherence as

$$P_S = 2g_{\text{off}}\text{Im}(\beta). \quad (\text{F6})$$

2. Current conservation laws

Overall, the time evolution of the local particle numbers n_L and n_R , set by

$$\dot{n}_j = \text{Tr}(\hat{n}_j \mathcal{D}_j \hat{\rho}) - i \text{Tr}([\hat{n}_j, H_I + H_J] \hat{\rho}), \quad (\text{F7})$$

with $j = L, R$, can be expressed as the following transport identities:

$$\dot{n}_L = I_L - I_S + P_S, \quad (\text{F8a})$$

$$\dot{n}_R = I_R + I_S + P_S. \quad (\text{F8b})$$

Substituting n_j by its transport-based expression, Eq. (4), one obtains the following equations on the internal and external transport quantities:

$$I_S = \frac{1}{2} \left(\frac{\dot{I}_L}{\Gamma_L} + I_L - \frac{\dot{I}_R}{\Gamma_R} - I_R \right), \quad (\text{F9a})$$

$$P_S = -\frac{1}{2} \left(\frac{\dot{I}_L}{\Gamma_L} + I_L + \frac{\dot{I}_R}{\Gamma_R} + I_R \right). \quad (\text{F9b})$$

This identity exactly corresponds to Eq. (8). Similarly, deriving in time Eq. (F3)-(F6), yields

$$\dot{I}_S = -\frac{\Gamma}{2} I_S - 2g_I \delta \text{Re}(\alpha) - 2g_I^2 \left(\frac{I_L - \gamma_L^+}{\Gamma_L} - \frac{I_R - \gamma_R^+}{\Gamma_R} \right), \quad (\text{F10a})$$

$$\dot{P}_S = -\frac{\Gamma}{2} P_S + 2g_J E \text{Re}(\beta) + 2g_J^2 \left(1 + \frac{I_L - \gamma_L^+}{\Gamma_L} + \frac{I_R - \gamma_R^+}{\Gamma_R} \right), \quad (\text{F10b})$$

a variant of Eq. (9).

In conclusion, the tomography technique proposed in this work is based on the following set of correspondences: the current averages I_L and I_R directly determine the populations n_L and n_R ; their time derivatives \dot{I}_L and \dot{I}_R provides information on the imaginary coherences $\text{Im}(\alpha)$ and $\text{Im}(\beta)$ via the internal particle current and production I_S and P_S ; and finally, the second time derivatives \ddot{I}_L and \ddot{I}_R are linked with the the real coherences $\text{Re}(\alpha)$ and $\text{Re}(\beta)$ thanks to the time-derivation of I_S and P_S .

In the steady-state, current conservation identities in each qubit lead to the equations:

$$I_S^{ss} = (I_L^{ss} - I_R^{ss})/2, \quad (\text{F11a})$$

$$P_S^{ss} = -(I_R^{ss} + I_S^{ss})/2. \quad (\text{F11b})$$

The steady-state internal current I_S^{ss} is thus equal to the average current flowing from the left to the right reservoir, while the steady-state internal production P_S^{ss} counterbalances the average release of particles out of the system.

Appendix G: Transport-based entanglement measures

In this section, we provide the complete expression of the concurrence at all times in terms of transport observables. Starting from an initial X-shaped density matrix, the concurrence is given at all time by:

$$\mathcal{C} = 2 \max\{0, |\alpha| - \sqrt{r_{00}r_{11}}, |\beta| - \sqrt{r_{01}r_{10}}\} \quad (\text{G1})$$

where

$$|\alpha| - \sqrt{r_{00}r_{11}} = \frac{1}{|2g_{\text{res}}|} \sqrt{(\varphi_L - \varphi_R)^2 + \frac{1}{\delta^2} (\dot{\varphi}_L - \dot{\varphi}_R + \frac{\tilde{\Gamma}}{2} (\varphi_L - \varphi_R) + 4g_{\text{res}}^2 (\chi_L - \chi_R))^2} - \frac{1}{\Gamma_L \Gamma_R} \sqrt{\left(S_{LR} + (I_L - \gamma_L^+) (I_R - \gamma_R^+) \right) \left(S_{LR} + (I_L + \gamma_L^-) (I_R + \gamma_R^-) \right)} \quad (\text{G2})$$

and

$$|\beta| - \sqrt{r_{01}r_{10}} = \frac{1}{|2g_{\text{off}}|} \sqrt{(\varphi_L + \varphi_R)^2 + \frac{1}{E^2} (\dot{\varphi}_L + \dot{\varphi}_R + \frac{\tilde{\Gamma}}{2}(\varphi_L + \varphi_R) + 4g_{\text{off}}^2(\chi_L + \chi_R + 1))^2} - \frac{1}{\Gamma_L \Gamma_R} \sqrt{\left(S_{LR} + (I_L - \gamma_L^+)(I_R + \gamma_R^-)\right) \left(S_{LR} + (I_L + \gamma_L^-)(I_R - \gamma_R^+)\right)} \quad (\text{G3})$$

with $\varphi_j(t) = \frac{I_j(t)}{\Gamma_j} + I_j(t)$ and $\chi_j(t) = \frac{I_j(t) - \gamma_j^+}{\Gamma_j}$. For the sake of clarity, time-dependence is implicit here.